

RESEARCH ARTICLE

A unified description of sum-frequency-generation, parametric-down-conversion and two-photon-fluorescence.

Oleksiy Roslyak* & Shaul Mukamel**
 Email: *oroslyak@uci.edu, **smukamel@uci.edu

Chemistry Department, University of California, Irvine, California 92697-2025, USA

(January 11, 2009)

A superoperator nonequilibrium Green's function (SNGF) formalism is presented for computing nonlinear optical processes involving any combination of classical and quantum optical modes. Closed correlation-function expressions based on superoperator time-ordering are derived for the combined effects of causal response and non-causal spontaneous fluctuations. Coherent three wave mixing (sum frequency generation (SFG) and parametric down conversion (PDC)) involving one and two quantum optical modes respectively, are connected to their incoherent counterparts: two-photon-induced fluorescence (TPIF) and two-photon-emitted fluorescence (TPEF).

Keywords: PDC, TPF, SFG, DFG, generalized response functions

Much effort in quantum optics has been primarily focused on the quantum properties of light [1–3]. When the optical fields are tuned off-resonance with respect to the matter transitions, the matter serves as mediator of interactions between the field modes. The optical processes may then be described by an effective Hamiltonian for the field [1, 2] and the matter enters only through some parameters such as n^{th} -order nonlinear susceptibilities $\chi^{(n)}$. The parametric description quantum of optics misses all resonant spectroscopic information.

Non-linear spectroscopy, on the other hand, is mainly concerned with intrinsic properties of the material and uses classical light to interrogate them [4, 5]. The semiclassical approach [2] which treats the material quantum mechanically and all fields classically is broadly used in spectroscopic applications. When a quantum system interacts with a classical field its properties may be described by a set of *causal response functions* (CRF) which can be derived order by order in the coupling. These CRF are given by specific combinations of dipole correlation functions with various time orderings [4]. Causality which implies that all interactions occur prior to the observation time is guaranteed by their retarded nature. Strictly speaking, for spontaneous processes where the signal field is initially in the vacuum state, that mode must be treated quantum mechanically. This is avoided in the semiclassical approach to coherent nonlinear optics by computing the signal by solving Maxwell's equations; quantum fields are never introduced at this level of theory.

Quantum spectroscopy brings both worlds together by treating the light and matter as coupled quantum systems. When two quantum systems are placed in contact, they interact thorough spontaneous, non-causal, fluctuations. It is not possible to classify the dynamical events in terms of a cause and effect. Such systems

can be described by combinations of correlation functions other than the CRF known as multi-point Green's functions[6, 7]. By working in Liouville space and introducing superoperator notation it is possible to describe processes involving any combination of classical and quantum optical modes in terms of a single set of superoperator non-equilibrium Green's functions (SNGF)[6, 8, 9].

In this paper we apply the SNGF formalism to establish the connections between various types of experiments involving quantum modes of the radiation field. All quantum modes considered here are initially in their vacuum states and are populated by spontaneous emission. Spectroscopy with other types of the non-classical quantum fields including entangled photons will be reported elsewhere.

We first consider several coherent signals [8] which scale as $N(N - 1)$, where N is the number of optically active molecules. These include homodyne-detected sum frequency generation (SFG)[10] and difference frequency generation (DFG)[4, 11] which involve two classical and one quantum mode. We further calculate parametric down conversion (PDC)[12–15] which involves one classical and two quantum modes. PDC is one of the primary sources of entangled photon pairs [1, 16, 17].

We next consider incoherent signals which scale as N . These comprise heterodyne detected SFG and DFG, which involve three classical modes, and two types of two photon fluorescence [18]: two photon induced fluorescence with one classical and two quantum modes (TPIF)[19–21] and two photon emitted fluorescence with two classical and one quantum mode (TPEF).

The SNGF formalism is essential when some modes other than the signal mode are quantum. Once the quantum nature of the optical field is taken into account, the signals may not be represented solely by the CRF's since non-causal correlated spontaneous fluctuations of *both* matter of field must be taken into account. Optical signals can then be described by superoperator non-equilibrium Green's functions (SNGF) which are given by other combinations of dipole correlation functions.

The semiclassical approach cannot describe the most general non-linear optical processes which involve spontaneously generated photons. The SNGF language of quantum spectroscopy can describe both quantum and classical optical fields. Seemingly different processes can then be treated by a unified formalism.

The SNGF allow us to classify the various possible measurement systematically and compare their information content. This formalism has been applied to describe Van Der Waals forces in molecules[6], charge transfer in quantum junctions [7] and inelastic resonances in STM currents [22]. A brief description of the SNGF is presented in the following section.

1. Quantum description of multiple wave mixing.

We start with the quantized light-matter Hamiltonian

$$H(t) = H_0 + H_{int}(t) \quad (1)$$

Here H_0 is the material Hamiltonian. The field-matter coupling in the interaction picture with respect to the optical field is given by

$$H_{int} = - \sum_{\alpha} E'_{\alpha}(t) V'_{\alpha}$$

The quantized electric field operator of mode α is given by:

$$E'_{\alpha}(t) = E_{\alpha}(t) + E_{\alpha}^{\dagger}(t) \quad (2)$$

Here

$$E_\alpha(t) = \mathbf{e}_\alpha \sqrt{\frac{2\pi\hbar\omega_\alpha}{\Omega}} a_\alpha \exp(i\mathbf{k}_\alpha \mathbf{r} - i\omega_\alpha t)$$

is the positive frequency part and $\mathbf{e}_\alpha, \omega_\alpha, \mathbf{k}_\alpha$ are the polarization, frequency and wave vector of the given mode α ; a_α is the photon annihilation operator; Ω is the quantization volume. The mode index spans a set $\alpha = \{|n\rangle_1, |n\rangle_2 \dots\}$, where $|n\rangle_\alpha$ is an n photon state of in mode α . Similar to equation (2), the molecular transition dipole moment operator will be partitioned into positive and negative frequency components $V'_\alpha = V_\alpha + V_\alpha^\dagger$, where the subscript implies projection on the quantized electric field direction of mode α .

We assume that the detector registers the number of photons per unit time in mode α and the signal is given by the time averaged photon flux:

$$S_\alpha = \lim_{T \rightarrow \infty} \frac{1}{2T} \int_{-T}^T \frac{d}{dt} \langle a_\alpha^\dagger a_\alpha \rangle dt \quad (3)$$

Using the Heisenberg equation of motion for the photon number in mode α :

$$\frac{d}{dt} a_\alpha^\dagger a_\alpha = \frac{i}{\hbar} [H_{int}, a_\alpha^\dagger a_\alpha],$$

and the interaction Hamiltonian (1), the signal can be expressed as:

$$S_\alpha = \frac{1}{\pi\hbar} \Im \int_{-\infty}^{\infty} \langle E'_\alpha(t) V'_\alpha(t) \rangle dt \quad (4)$$

where the explicit time dependence of the dipole operator is given in the interaction picture with respect to the molecular part of the Hamiltonian H_0 [8]. The expectation value $\langle \dots \rangle$ is over the initial state of the entire system (matter + photons) at $t = -\infty$.

We next introduce the superoperator notation. With every ordinary operator A we associate two superoperators defined by their action on an ordinary operator X as $A_L = AX$ (left), $A_R = XA$ (right). We further define a different set of superoperators by a unitary transformation: $A_- = \frac{1}{\sqrt{2}}(A_L - A_R)$, $A_+ = \frac{1}{\sqrt{2}}(A_L + A_R)$. More details on the superoperator algebra in the L, R and the $+, -$ representations are given in Appendix A [22].

The SNGF of n^{th} order are defined as traces of time ordered products of such superoperators: $\langle \mathcal{T} A_+(t) \underbrace{A_+(t_n) \dots A_+(t_{n-m+1})}_m \underbrace{A_-(t_{m-n}) \dots A_-(t_1)}_{n-m} \rangle$, where

$m = 0, \dots, n$. The time ordering superoperator a key bookkeeping device in this formalism and is defined as:

$$\begin{aligned} \mathcal{T} A_{\nu_1}(t_2) B_{\nu_2}(t_1) &= \theta(t_2 - t_1) A_{\nu_1}(t_2) B_{\nu_2}(t_1) + \\ &+ \theta(t_1 - t_2) B_{\nu_2}(t_1) A_{\nu_1}(t_2) \end{aligned}$$

The indices ν_j can be either $+$ or $-$; $\theta(t)$ is the Heaviside step function. The SNGF's may contain an arbitrary number of $+$ and $-$ superoperators. The chronologically last superoperator must be a $+$ one, otherwise the SNGF vanishes (See

eq.(A3)).

The signal (4) can be expanded perturbatively $S_\alpha = \sum_{m=1}^{\infty} S_\alpha^{(m)}$ in the interaction superoperator H_-^{int} (See Appendix A). The material SNGF's are defined as:

$$\mathbb{V}_{\nu_{m+1}\nu_m\dots\nu_1}^{(m)}(t_{m+1}, t_m, \dots, t_1) = \langle \mathcal{T} V'_{\nu_{m+1}}(t_{m+1}) V'_{\nu_m}(t_m) \dots V'_{\nu_1}(t_1) \rangle \quad (5)$$

The causal response functions (CRF) are one type of SNGF and have the form of $\langle A_+(t) A_-(t_n) \dots A_-(t_1) \rangle$ (one + and several - superoperators). SNGF's of the form $\mathbb{V}_{\underbrace{+-\dots-}_m}^{(m)}$ give causal ordinary molecular response function of m^{th} order. The

material SNGF of the form $\mathbb{V}_{\underbrace{++\dots+}_m}^{(m)}$ represent the m^{th} moment of the fluctuating

molecular superoperator. Material SNGF of the form $\mathbb{V}_{\underbrace{++\dots+}_n \underbrace{-\dots-}_{m-n}}^{(m)}$ indicates

changes in n^{th} moment of molecular fluctuations induced by $m - n$ light/matter interactions[6].

The optical field SNGF's are similarly defined:

$$\mathbb{E}_{\nu_{m+1}\nu_m\dots\nu_1}^{(m)}(t_{m+1}, t_m, \dots, t_1) = \langle \mathcal{T} E'_{\nu_{m+1}}(t_{m+1}) E'_{\bar{\nu}_m}(t_m) \dots E'_{\bar{\nu}_1}(t_1) \rangle \quad (6)$$

The m wave mixing signal is given by a sum of 2^m terms, each factorized into a product of m^{th} order material and corresponding optical field SNGF's:

$$S_\alpha^{(m)} = \mathfrak{S} \frac{i^m 2^{(m+1)/2} \delta_{m+1,\alpha}}{\pi m! \hbar^{m+1}} \sum_{\nu_m} \dots \sum_{\nu_1} \int_{-\infty}^{\infty} dt_{m+1} dt_m \dots dt_1 \times \quad (7)$$

$$\Theta(t_{m+1}) \mathbb{V}_{\nu_{m+1}\nu_m\dots\nu_1}^{(m)}(t_{m+1}, t_m, \dots, t_1) \mathbb{E}_{\nu_{m+1}\bar{\nu}_m\dots\bar{\nu}_1}^{(m)}(t_{m+1}, t_m, \dots, t_1)$$

where t_{m+1}, t_m, \dots, t_1 are the light/matter interaction times. The factor $\Theta(t_{m+1}) = \prod_{i=1}^m \theta(t_{m+1} - t_i)$ guarantees that the t_{m+1} is the last light-matter interaction. The indexes $\bar{\nu}_j$ are the conjugates to ν_j and are defined as follows: the conjugate of + is - and vice versa. Equation (7) implies that each material excitation is caused by fluctuations in the optical field and vice versa. The $2^{(m+1)/2}$ factor comes from the relation (A1) between the commutator(anti-commutator) and the superoperators.

Equation (7) also holds in the L, R representation, where the conjugate of "left" is "left" and the conjugate of "right" is "right": $\bar{L} = L, \bar{R} = R$. In this representation the coefficient $2^{(m+1)/2}$ must be replaced by unity. The material SNGF $\mathbb{V}_{\underbrace{L\dots L}_n \underbrace{R\dots R}_{m-n}}^{(m)}$ represent a *Liouville space pathway* with $n + 1$ interactions from

the left (i.e. with the ket) and $m - n$ interactions from the right (i.e. with the bra).

We next recast the material SNGF (5) in the frequency domain by performing a

multiple Fourier transform:

$$\begin{aligned} \chi_{\nu_{m+1}\nu_m\dots\nu_1}^{(m)}(-\omega_{m+1};\omega_m,\dots,\omega_1) = & \quad (8) \\ & \int_{-\infty}^{\infty} dt_{m+1}\dots dt_1 \Theta(t_{m+1}) e^{i(\omega_m t_m + \dots + \omega_1 t_1)} \\ & \delta(-\omega_{m+1} + \omega_m + \dots + \omega_1) \mathbb{V}_{\nu_{m+1}\nu_m\dots\nu_1}^{(m)}(t_{m+1}, t_m, \dots, t_1) \end{aligned}$$

The SNGF $\chi_{\underbrace{+\dots-}_m}^{(m)}(-\omega_{m+1};\omega_m,\dots,\omega_1)$ (with one + and the rest $m -$ indices)

are the m^{th} order nonlinear susceptibilities derived from CRF's. Other SNGF's in the frequency domain with arbitrary combination of + and - indices can be interpreted similarly to their time domain counterparts (5).

In the L, R representation, each material SNGF (8) represents a Liouville-space pathways. For some techniques it is more convenient to use a mixed representation of SNGF where some superoperators are in the L, R and others in the +, - representation.

In the coming sections the general formal expression for the signal (7) will be applied to calculate specific non-linear techniques by a proper choice of initial conditions for the optical field and the allowed material optical transitions.

2. Heterodyne-detected sum and difference frequency generation.

We first consider two second order signals $S_3^{(2)}$ involving three classical modes. The third mode is singled out since it is heterodyne detected and its time-averaged photon flux (number of photons per unit time) is measured.

The initial state of the field is given by a product of coherent states: $|t = -\infty\rangle = |\beta\rangle_1 |\beta\rangle_2 |\beta\rangle_3$, where $|\beta\rangle_\alpha$ are eigenfunctions of the mode α annihilation operator: $a_\alpha |\beta\rangle_\alpha = \beta_\alpha |\beta\rangle_\alpha$. Coherent states are the most classical quantum states of light [3].

For coherent optical states, all field SNGF in the L, R representation (6) are identical $E'_L = E'_R$ (the superoperator index makes no difference since all operations commute). In the +, - representation no "minus" indices are allowed, since $E'_- = 0$. Only one type of optical SNGF then contribute to the classical signal:

$$\mathbb{E}_{+++}^{(2)}(t_3, t_2, t_1) = \mathcal{E}'(t_3) \mathcal{E}'(t_2) \mathcal{E}'(t_1) \quad (9)$$

where $\mathcal{E}' = \langle E'_L \rangle = \langle E'_R \rangle = \beta_\alpha \sqrt{2\pi\hbar\omega_\alpha/\Omega}$ is the classical field amplitude.

The conjugate material SNGF's (5) transformed into L, R representation contains eight terms with only half of them being independent:

$$\begin{aligned} 2^{3/2} \mathbb{V}_{+--}^{(2)}(t_3, t_2, t_1) = & \mathbb{V}_{LLL}^{(2)}(t_3, t_2, t_1) - \mathbb{V}_{LRL}^{(2)}(t_3, t_2, t_1) - \\ & - \mathbb{V}_{LLR}^{(2)}(t_3, t_2, t_1) + \mathbb{V}_{LRR}^{(2)}(t_3, t_2, t_1) \end{aligned} \quad (10)$$

where we have put the last interaction to the left branch.

To simplify eq. (10) further, we assume a three level material scheme as shown in Fig.1(B) and Fig.2(B). All transitions between ground $|g\rangle$, intermediate $|e\rangle$ and $|f\rangle$ state manifolds are allowed. The dipole moment creation operator projected on

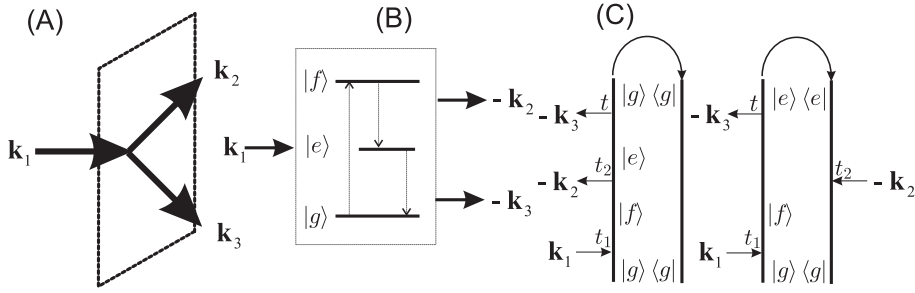


Figure 1. Heterodyne detected DFG: (A) phase matching condition $\mathbf{k}_3 = \mathbf{k}_1 - \mathbf{k}_2$; (B) molecular level scheme; (C) CTPL diagrams.

mode α is given by:

$$V_\alpha^\dagger = \mu_{ge}^\alpha |g\rangle\langle e| + \mu_{ef}^\alpha |e\rangle\langle f| + \mu_{gf}^\alpha |g\rangle\langle f| \quad (11)$$

with the corresponding optical transition dipole moments $\mu_{eg}^\alpha = \mathbf{e}^\alpha \langle e|\mu|g\rangle$, $\mu_{ef}^\alpha = \mathbf{e}^\alpha \langle f|\mu|e\rangle$, $\mu_{gf}^\alpha = \mathbf{e}^\alpha \langle f|\mu|g\rangle$. Initially the material system is in the ground state $|g\rangle$. Once the molecular level scheme is specified we shall invoke the rotating-wave approximation (RWA) for the interaction Hamiltonian:

$$H_{int} = - \sum_{\alpha} V_\alpha^\dagger E_\alpha(t) + c.c. \quad (12)$$

Without losing generality we assume that the last interaction is emission, which implies that $\mathbb{V}_{LRR}^{(2)}(t_3, t_2, t_1) \equiv 0$ since one can not de-excite the ground state.

In RWA the material SNGF's written in terms of L, R superoperators, can be represented by close-time path loop (CTPL) diagrams introduced by Schwinger-Keldysh many body theory [8, 9]. The rules for constructing these partially-time-ordered diagrams are summarized in Appendix B. All CTPL diagrams corresponding to material SNGF's (10) are shown in Fig.1(C) and Fig.2(C) (possible permutation of \mathbf{k}_2 and \mathbf{k}_1 is not shown but implied). The signals (7) are given by the causal $\chi_{+--}^{(2)}(-\omega_3, \pm\omega_2, \pm\omega_1)$ response functions. This result is well known and can be obtained by using the standard semiclassical approach taking the optical fields to be classical. This calculation illustrates how the SNGF formalism works.

To obtain non-linear signals (7), corresponding material SNGF (10) must be calculated for each technique. To that end we must to specify the phase matching conditions (frequencies and wave vectors of the optical modes). This will be done below.

2.1. Difference frequency generation (DFG)

In DFG (Fig.1) the first mode \mathbf{k}_1 promotes the molecule from its ground state $|g\rangle$ into state $|f\rangle$. The second mode \mathbf{k}_2 induces stimulated emission from $|f\rangle$ to an intermediate $|e\rangle$; and the third mode \mathbf{k}_3 stimulates the emission from $|e\rangle$ to $|g\rangle$. All optical modes are linearly polarized in \mathbf{e}_x direction. The signal is measured in the phase matching direction $\mathbf{k}_3 = \mathbf{k}_1 - \mathbf{k}_2$. The CTPL diagrams corresponding to this technique are shown in Fig.1(C).

The optical field SNGF in equation (9) is:

$$\mathbb{E}_{+++}^{(2)}(t_3, t_2, t_1) = \mathcal{E}_3^*(t) \mathcal{E}_2^*(t_2) \mathcal{E}_1(t_1) \quad (13)$$

The material SNGF's in equation (10) become:

$$\begin{aligned} 2^{3/2}\mathbb{V}_{+--}^{(2)}(t_3, t_2, t_1) &= \\ &= \langle \mathcal{T}V_L^3(t_3)V_L^{2,\dagger}(t_2)V_L^{1,\dagger}(t_1) - \langle \mathcal{T}V_L^3(t_3)V_R^{2,\dagger}(t_2)V_L^{1,\dagger}(t_1) \rangle = \\ &= \theta(t_2 - t_1)\langle V^3(t_3)V^{2,\dagger}(t_2)V^{1,\dagger}(t_1) - \langle V^{1,\dagger}(t_1)V_L^3(t_3)V^{2,\dagger}(t_2) \rangle \end{aligned} \quad (14)$$

Note that $\mathbb{V}_{LLR}^{(2)}(t_3, t_2, t_1) = 0$ since the molecule can not be de-excited from its ground state. The step function $\theta(t_2 - t_1)$ indicates that interactions within one branch are time ordered.

Substituting (14), (13) into (7), the DFG signal can be written in the frequency domain as:

$$S_{DFG}(-\omega_3, \omega_2, \omega_1) = \frac{2^{3/2}}{\pi\hbar} \Im \mathcal{E}_3^* \mathcal{E}_2^* \mathcal{E}_1 \chi_{+--}^{(2)}(-\omega_3; -\omega_2, \omega_1) \delta(\omega_1 - \omega_2 - \omega_3) \quad (15)$$

where second order susceptibility is give by:

$$\begin{aligned} 2^{3/2}\chi_{+--}^{(2)}(-(\omega_1 - \omega_2); -\omega_2, \omega_1) &= \\ &= \frac{1}{2!\hbar^2} (\langle g | V_3 G(\omega_g + \omega_1 - \omega_2) V_2 G(\omega_g + \omega_1) V_1^\dagger | g \rangle - \\ &\langle g | V_2 G^\dagger(\omega_g + \omega_1 - \omega_2) V_3 G(\omega_g + \omega_1) V_1^\dagger | g \rangle) \end{aligned} \quad (16)$$

Here $G(\omega)$ is the retarded Green's function:

$$G(\omega) = \frac{\hbar}{\hbar\omega - H_{mol} + i\hbar\gamma} \quad (17)$$

Advanced Green's function $G^\dagger(\omega)$ is its hermitian conjugate; $\hbar\gamma$ is the dephasing rate. Note that sinal (16) can be directly restored from the diagrams in Fig.1(C) simply by applying the rules given in Appendix B.

Expanding (17) into molecular eigenstates and putting into (16) gives:

$$\begin{aligned} 2^{3/2}\chi_{+--}^{(2)}(-(\omega_1 - \omega_2); -\omega_2, \omega_1) &= \\ &= \frac{1}{2!\hbar^2} \frac{\mu_{gf}^x \mu_{fe}^x \mu_{eg}^x}{(\omega_1 - \omega_{gf} + i\hbar\gamma_{gf})(\omega_1 - \omega_2 - \omega_{eg} + i\hbar\gamma_{eg})} - \\ &= \frac{1}{2!\hbar^2} \frac{\mu_{gf}^x \mu_{fe}^x \mu_{eg}^x}{(\omega_1 - \omega_{gf} + i\hbar\gamma_{gf})(\omega_2 - \omega_{eg} - i\hbar\gamma_{eg})} \end{aligned} \quad (18)$$

Equation (18) indicates that the signal induced by classical optical fields is given by the second order CRF. This susceptibility tensor is used in the standard effective interaction Hamiltonian of quantum optics (44).

2.2. Sum Frequency Generation SFG

In SFG (Fig.2 (A)) the first two modes promote the molecule from its ground state $|g\rangle$ through intermediate state $|e\rangle$ into the state $|f\rangle$. The third mode induces stimulated emission from $|f\rangle$ to the ground state $|g\rangle$. The signal is generated in the phase matching direction $\mathbf{k}_3 = \mathbf{k}_1 + \mathbf{k}_2$.

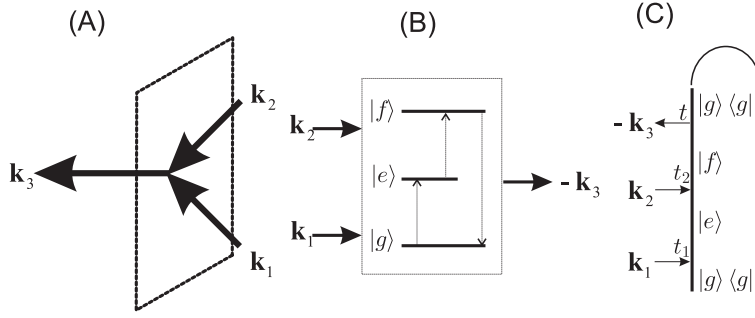


Figure 2. Heterodyne detected SFG: (A) phase matching condition $\mathbf{k}_3 = \mathbf{k}_1 + \mathbf{k}_2$; (B) level scheme; (C) CTPL diagrams.

The heterodyne SFG signal can be obtained as we did for DFG, by utilizing the diagrams shown in Fig.2(C):

$$S_{SFG}(\omega_1, \omega_2) = \frac{2^{3/2}}{\pi \hbar} \Im \mathcal{E}_3^* \mathcal{E}_2 \mathcal{E}_1 \chi_{+--}^{(2)}(-\omega_3; \omega_2, \omega_1) \delta(\omega_1 + \omega_2 - \omega_3) \quad (19)$$

The CRF is now given by:

$$\begin{aligned} & 2^{3/2} \chi_{+--}^{(2)}(-(\omega_1 + \omega_2); \omega_2, \omega_1) = \\ & \frac{1}{2! \hbar^2} \langle g | V_3 G(\omega_g + \omega_1 + \omega_2) V_2^\dagger G(\omega_g + \omega_1) V_1^\dagger | g \rangle = \\ & \frac{1}{2! \hbar^2} \frac{\mu_{ge}^x \mu_{fe}^x \mu_{eg}^x}{(\omega_1 - \omega_{eg} + i \hbar \gamma_{eg})(\omega_1 + \omega_2 - \omega_{gf} + i \hbar \gamma_{gf})} \end{aligned} \quad (20)$$

SFG with three classical waves can be alternatively described in Hilbert space by an effective interaction Hamiltonian (43) with the material parameter given by equation (20).

The purpose of this section was to illustrate how the superoperator approach works for well-known classical spectroscopic techniques. We started from the fact that all the optical modes are classical (coherent states) and therefore the signal is given by the CRF. In the SNGF's language it can be translated into the second order susceptibility $\chi_{+--}^{(2)}$. All moments of molecular fluctuations vanish identically ($\chi_{++-}^{(2)} = \chi_{+++}^{(2)} = 0$). From the $+$, $-$ representation we transformed the CRF to L, R representation and implied CTPL diagrams technique to find relevant molecular Liouville pathways and restore the signals.

In the coming sections equations (20) and (18) will be compared with other techniques involving various combinations of quantum and classical optical fields. We apply described above algorithm backwards. That is for each individual technique we establish non-vanishing Liouville pathways in the L, R representation and transform the signal to $+$, $-$ representation. That representation will tell us to what degree the molecular fluctuations determine the signals.

3. Two-photon-induced fluorescence (TPIF) vs. homodyne SFG

We now turn to techniques involving two classical and one quantum mode where the initial state of the optical field is: $|t = -\infty\rangle = |\beta_1\rangle_1 |\beta_2\rangle_2 |0\rangle_3$. We again assume the three level material system (Fig.3(B)). We assume that the ground state is a manifold and $\omega_{eg} \neq \omega_{ef}$. Latter allows us to focus on the resonant SNGF's and reduces the number of diagrams.

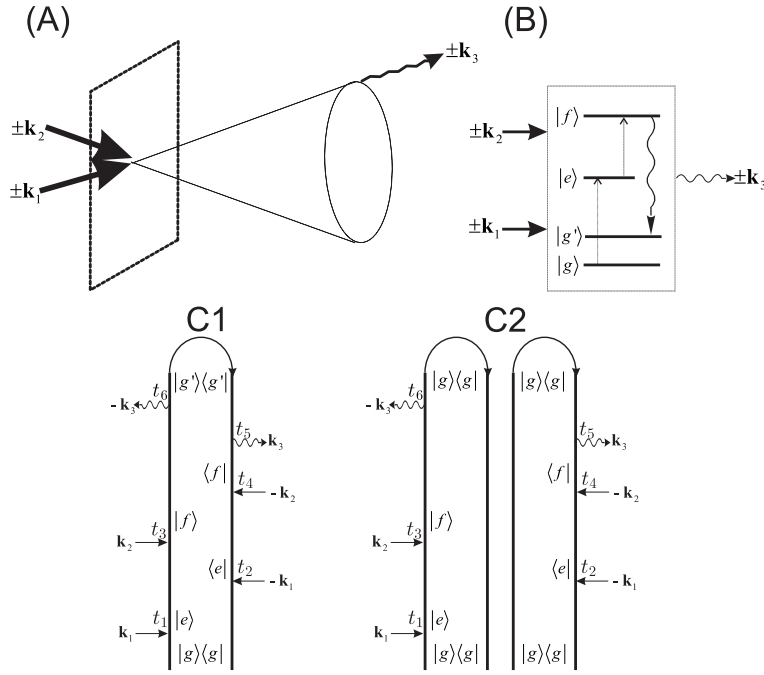


Figure 3. Three wave process with two classical and one quantum mode. (A) phase-matching conditions: for TPIF the spontaneous mode is not particularly directed, but for the homodyne-detected SFG the mode is emitted into a cone determined by the reciprocal of the sample size. (B) molecular level scheme; (C1) CTPL for the incoherent TPIF; (C2) is for the coherent homodyne-detected SFG. For the coherent signal, optical field interactions with the molecule 1 of the pair occur from the left (L), and the interactions with the molecule 2 occur from the right (R).

The two classical modes \mathbf{k}_1 , \mathbf{k}_2 promote the molecule from its ground state $|g\rangle$ through the intermediate state $|e\rangle$ into the final state $|f\rangle$. The system then spontaneously moves back into the ground state manifold $|g'\rangle$ by emitting a photon into the third detected mode \mathbf{k}_3 which is initially in the vacuum state (See Fig.3 (B)).

The signal (photon flux in the \mathbf{k}_3 mode) involves three optical field modes and six light/matter interactions. Therefore, equation (7) must be expanded to fifth order in H_{int} .

The fifth order signal $S_{CCQ}^{(5)}$ (CCQ implies two classical and one quantum mode) may be written as sum of 2^5 terms each given by a product of molecule/field six point SNGF's. Only processes which satisfy the following conditions contribute to the signal:

- (1) Creation operator of the quantum mode a_3^\dagger must be accompanied by corresponding annihilation operator a_3 .
- (2) The quantum mode can only de-excite the molecule (emission), which implies that the annihilation operator must act on the bra and the creation operator act on the ket.
- (3) The coherent optical fields are tuned off resonance with respect to the $\omega_{fg'}$ transition. Hence, the signal is not masked by stimulated emission.

We assume a collection of N noninteracting molecules positioned at \mathbf{r}_i so that $V = \sum_i V_i \delta(\mathbf{r} - \mathbf{r}_i)$. The relevant CTPL diagrams for processes involving three optical modes and six light/matter interactions are presented in Fig.3(C). The field modes can either interact with the same molecule (incoherent process, Fig.3(C1)) or two different molecules (coherent process, Fig.3(C2))[8].

3.1. Two-photon-induced fluorescence (TPIF)

TPIF is an incoherent three wave process involving two classical and one quantum mode. The phase-matching condition $\mathbf{k}_1 - \mathbf{k}_1 + \mathbf{k}_2 - \mathbf{k}_2 + \mathbf{k}_3 - \mathbf{k}_3 = 0$ is automatically satisfied for any \mathbf{k}_3 . The actual angular disposition of the spontaneously emitted photons is determined by eq. (26) and electric field vectors of the input, subject to rotational diffusion over the two-photon excited state lifetime. Using the identity $\sum_{i=1}^N \exp i(\mathbf{k}_1 - \mathbf{k}_1 + \mathbf{k}_2 - \mathbf{k}_2 + \mathbf{k}_3 - \mathbf{k}_3)(\mathbf{r} - \mathbf{r}_i) = N$ we obtain the optical field SNGF (6):

$$\begin{aligned} \mathbb{E}_{LR++++}^{(5)}(t_6, t_5, \dots, t_1) = \\ N \mathcal{E}_1(t_1) \mathcal{E}_1^*(t_2) \mathcal{E}_2(t_3) \mathcal{E}_2^*(t_4) \frac{2\pi\hbar\omega_3}{\Omega} \exp(i\omega_3(t_6 - t_5)) \end{aligned} \quad (21)$$

The relevant material SNGF (5) is:

$$\begin{aligned} \mathbb{V}_{LR-----}^{(5)}(t_6, t_5, \dots, t_1) = \\ \langle T V_L^3(t_6) V_R^{3,\dagger}(t_5) V_-^2(t_4) V_-^{2,\dagger}(t_3) V_-^1(t_2) V_-^{1,\dagger}(t_1) \rangle \end{aligned} \quad (22)$$

Utilizing equations (21) and (22), the frequency domain signal can be written as:

$$\begin{aligned} S_{TPIF}(\omega_1, \omega_2) = \frac{N}{\pi\hbar} \sum_{\mathbf{k}_3} |\mathcal{E}_1|^2 |\mathcal{E}_2|^2 \frac{8\pi\hbar\omega_3}{\Omega} \times \\ \mathfrak{S} \chi_{LR-----}^{(5)}(-\omega_3; \omega_3, -\omega_2, \omega_2, -\omega_1, \omega_1) \end{aligned} \quad (23)$$

Note that the above expression is given in the mixed ($L/R, +/-$) representation. It can be recast into the $+, -$ representation using the following identity:

$$2\chi_{LR-----}^{(5)} = \chi_{++++-----}^{(5)} - \chi_{+-----}^{(5)} \quad (24)$$

Here the first term (two "plus" four "minus" indices) arises since one of the modes is not classical. The second term is the ordinary CRF.

The material SNGF in the frequency domain (8) can be calculated by switching to the L, R representation:

$$\chi_{LR-----}^{(5)}(-\omega_3; \omega_3, -\omega_2, \omega_2, -\omega_1, \omega_1) = \frac{1}{4} \chi_{LRLRLR}^{(5)}(-\omega_3; \omega_3, -\omega_2, \omega_2, -\omega_1, \omega_1)$$

and utilizing the the diagram (C1) of Fig.3:

$$\begin{aligned} \chi_{LRLRLR}^{(5)}(-\omega_3; \omega_3, -\omega_2, \omega_2, -\omega_1, \omega_1) = \\ \frac{1}{5!\hbar^5} \langle g | V_1 G^\dagger(\omega_g + \omega_1) V_2 G^\dagger(\omega_g + \omega_1 + \omega_2) \times \\ \times V_3^\dagger G^\dagger(\omega_g + \omega_1 + \omega_2 - \omega_3) V_3 G(\omega_g + \omega_1 + \omega_2) V_2^\dagger G(\omega_g + \omega_1) V_1^\dagger | g \rangle \end{aligned} \quad (25)$$

Expanding equation (25) in molecular states gives:

$$4\chi_{LR}^{(5)}(-(\omega_1 + \omega_2); \omega_2, \omega_1) = \sum_{gg'} |\mu_{g'f}^x \mu_{fe}^x \mu_{eg}^x|^2 \quad (26)$$

$$\times \frac{1}{5! \hbar^5} \frac{1}{[(\omega_1 - \omega_{eg})^2 + \gamma_{eg}^2][\omega_1 + \omega_2 - \omega_{fg} + i\gamma_{fg}]}$$

$$\times \frac{1}{[\omega_1 + \omega_2 - \omega_{fg'} - i\gamma_{fg'}][\omega_1 + \omega_2 - \omega_3 - \omega_{gg'} - i\gamma_{gg'}]}$$

Provided the energy splitting within the ground state manifold $\omega_{gg'}$ is small compared with the optical transitions the signal can be recast in the form:

$$S_{TPIF}(\omega_1, \omega_2) = \frac{2N\omega_3}{5! \hbar^5 \Omega} |\mathcal{E}_1|^2 |\mathcal{E}_2|^2 |T_{g'g}(\omega_1, \omega_2)|^2 \delta(\omega_1 + \omega_2 - \omega_3 - \omega_{gg'}) \quad (27)$$

The transition amplitude is:

$$T_{g'g}(\omega_1, \omega_2) = \frac{\mu_{g'f} \mu_{fe} \mu_{eg}}{(\omega_1 - \omega_{eg} + i\gamma_{eg})(\omega_1 + \omega_2 - \omega_{fg} + i\gamma_{fg})}$$

is a direct generalization of the Kramers-Heisenberg form of ordinary (single-photon) fluorescence [4, 8].

The SNGF in equation (25) has been referred to as the fluorescence quantum efficiency by Webb [19] or the two-photon tensor by Callis [20]. Our result is identical to that of Callis.

When the two classical coherent modes are degenerate ($\omega_1 = \omega_2$) the signal in equation (27) describes non-resonant Hyper-Raman scattering ($\omega_{gg'} \neq 0$) also known as incoherent second harmonic inelastic scattering [20, 23, 24]. When $\omega_1 = \omega_2$ and $\omega_{gg'} \rightarrow 0$ (but not equal to) equation (27) describes off-resonant Hyper-Rayleigh scattering also known as incoherent second harmonic elastic scattering. Off-resonant Hyper-scattering is a major complicating factor for TPIF microscopy [25]. The distinction between Hyper-Raman and TPIF processes is complete analogy to their single photon counterparts (ordinary Raman and fluorescence). Latter has been discussed in details in Ref.[4]. The difference between this process can be described by adding pure dephasing processes. The concept of pure dephasing is beyond CTPL treatment.

3.2. Homodyne-detected sum frequency generation

The coherent part of the $S_{CCQ}^{(5)}$ signal ((C2) in Fig.3) describes homodyne-detected SFG. Photons in the \mathbf{k}_3 mode are spontaneously emitted into a cone [1] of solid angle $\sim \Delta\mathbf{k}$. Here the phase matching $\Delta\mathbf{k} \approx \mathbf{k}_1 + \mathbf{k}_2 - \mathbf{k}_3$ reflects the uncertainty in the phase given by the reciprocal of the sample characteristic size. For a large sample one can assume $\Delta\mathbf{k} \approx 0$ which effectively narrows the optical cone. The optical field SNGF is given by equation (21), but instead of factor N it now contains the factor:

$$\sum_{i=1}^N \sum_{j \neq i}^{N-1} e^{i\Delta\mathbf{k}(\mathbf{r}-\mathbf{r}_i)} e^{-i\Delta\mathbf{k}(\mathbf{r}-\mathbf{r}_j)} \approx N(N-1) \quad (28)$$

For large N the coherent part $\sim N(N - 1)$ dominates over the incoherent $\sim N$ response. For a small sample size, exact calculation of the optical field part of the SNGF is rather lengthy, but can be performed in the same fashion as done by Hong and Mandel [13] for the probability of photon detection.

Next we turn to the material SNGF. For the coherent process we must work in the joint space of two molecules $| \rangle_{1,2} = | \rangle_1 | \rangle_2$ interacting with the same field mode. Hence, the material SNGF of the joint system can be factorized into a product of SNGF of molecule 1 and 2:

$$\begin{aligned} \mathbb{V}_{LR-----}^{(5)}(t_6, t_5, \dots, t_1) = & \quad (29) \\ \langle \mathcal{T} V_+^3(t_6) V_+^{3,\dagger}(t_5) V_-^2(t_4) V_-^{2,\dagger}(t_3) V_-^1(t_2) V_-^{1,\dagger}(t_1) \rangle = & \\ \langle \mathcal{T} V_+^3(t_6) V_-^{2,\dagger}(t_3) V_-^{1,\dagger}(t_1) \rangle_1 \langle \mathcal{T} V_+^{3,\dagger}(t_5) V_-^2(t_4) V_-^1(t_2) \rangle_2 & \end{aligned}$$

where we have used the fact that the last interaction must be a "plus" and the field interactions with the two molecules are not time ordered.

Using equation (29) the coherent material SNGF in the frequency domain assumes the form of square of a second order CRF:

$$2^{6/2} \Im \chi_{++++}^{(5)}(-\omega_3; \omega_3, -\omega_2, \omega_2, -\omega_1, \omega_1) = \left| 2^{3/2} \chi_{+--}^{(2)}(-(\omega_1 + \omega_2); \omega_2, \omega_1) \right|^2$$

This factorization can be also obtained in the L, R representation using the diagram (C2) in Fig.3. The classical modes excite the molecules and the quantum mode de-excites them. Hence, the interactions with the first molecule ket (L) are accompanied by the conjugate interactions with the second molecule bra (R). Transforming the first molecule diagram to the $+, -$ representation we find that first molecule contributes the causal response $\chi_{LLL}^{(2)}(-(\omega_1 + \omega_2); \omega_2, \omega_1) = 2^{3/2} \chi_{+--}^{(2)}(-(\omega_1 + \omega_2); \omega_2, \omega_1)$ given by equation (20). The second molecule provides the conjugate causal response.

The homodyne-detected SFG signal is finally given by:

$$S_{SFG} = N(N - 1) |\mathcal{E}_1|^2 |\mathcal{E}_2|^2 \frac{2(\omega_1 + \omega_2)}{\Omega} \left| 2^{3/2} \chi_{+--}^{(2)}(-(\omega_1 + \omega_2); \omega_2, \omega_1) \right|^2 \quad (30)$$

Equation (30) can be alternatively obtained from the effective interaction Hamiltonian of the form (43) where the material parameter given by the causal response function $\chi_{+--}^{(2)}(-(\omega_1 + \omega_2); \omega_2, \omega_1)$.

Both homodyne and heterodyne SFG are given by the same CRF $\chi_{+--}^{(2)}$. The main difference is that the latter satisfies perfect phase matching condition, while for the former this condition is only approximate and becomes exact for sufficiently large samples.

To summarize this section we give the total signal for a three wave process involving two classical and one quantum field (CCQ) which includes both the

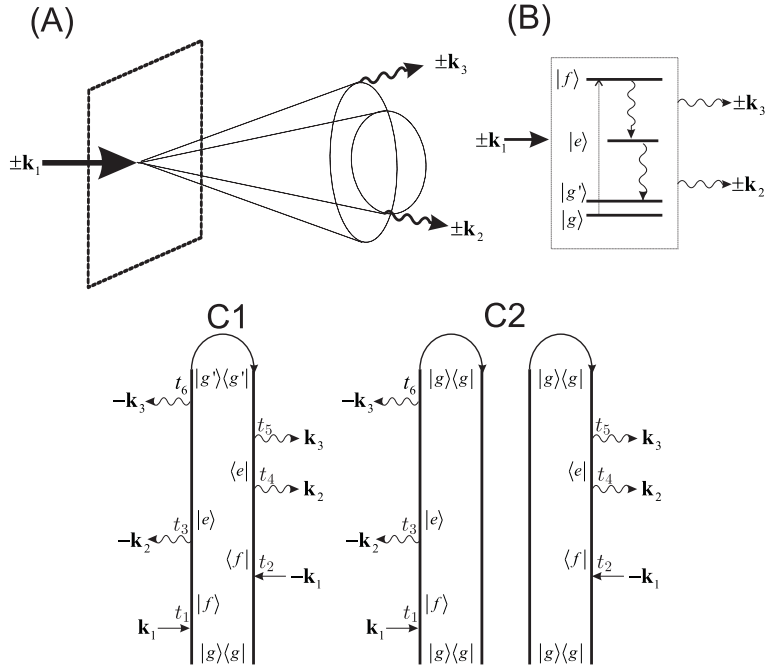


Figure 4. Three wave process with two quantum and one classical modes. (A) phase-matching conditions: for TPEF spontaneous modes are not directed, but for PDC the modes are emitted into two collinear cones. (B) molecular level scheme. CTPL for the incoherent TPEF (C1) and coherent Type I PDC (C2). In panel (C2) the two diagrams correspond to the conjugate pathways of the molecules in the pair.

incoherent and coherent components:

$$\begin{aligned}
 S_{CCQ}^{(5)}(\omega_2, \omega_1) &= |\mathcal{E}_1|^2 |\mathcal{E}_2|^2 \frac{2\omega_3}{\Omega} \quad (31) \\
 &[N2^{6/2} \Im \chi_{++++}^{(5)}(-\omega_3; \omega_3, -\omega_2, \omega_2, -\omega_1, \omega_1) - \\
 &-N2^{6/2} \Im \chi_{+-----}^{(5)}(-\omega_3; \omega_3, -\omega_2, \omega_2, -\omega_1, \omega_1) + \\
 &+N(N-1) \left| 2^{3/2} \delta(\omega_3 - \omega_1 - \omega_2) \chi_{+---}^{(2)}(-\omega_3; \omega_2, \omega_1) \right|^2]
 \end{aligned}$$

4. Two-photon-emitted fluorescence (TPEF) and Type I parametric down conversion (PDC).

We now turn to three wave processes involving one classical and two quantum modes (Fig.4). We start with the incoherent response of N identical molecules initially in their ground state and the initial state of the optical field is $|t = -\infty\rangle = |\beta_1\rangle_1 |0\rangle_2 |0\rangle_3$. The classical field \mathbf{k}_1 pumps the molecule from its ground state $|g\rangle$ into the excited state $|f\rangle$. The system then spontaneously emits two photons into modes \mathbf{k}_2 , \mathbf{k}_3 (See Fig.4 (B)) which are initially in the vacuum state. These incoherent process which involves one classical and two quantum modes will be denoted as two-photon-emitted fluorescence (TPEF).

This process is phase insensitive since the phase matching condition $\mathbf{k}_1 - \mathbf{k}_1 + \mathbf{k}_2 - \mathbf{k}_2 + \mathbf{k}_3 - \mathbf{k}_3 = 0$ is automatically satisfied for any \mathbf{k}_3 . Later we shall compare it with Type I parametric down conversion (PDC). Therefore, we chose the following beam polarization configuration as is usually done for PDC of this type: the spontaneously generated photons are polarized along x axis, and the classical mode polarized along y axis.

The TPEF signal is given by the time-averaged photon flux in the \mathbf{k}_3 mode. We

again make use of the CTPL diagrams to find the relevant SNGF contributing to the signal. Using the initial state of the field the diagrams must satisfy the following conditions:

- (1) Creation operators of the spontaneously generated modes a_3^\dagger, a_2^\dagger acting on the ket must be accompanied by corresponding annihilation operators a_3, a_2 acting on the bra.
- (2) The first mode $\omega_1(\mathbf{k}_1)$ is off-resonance with respect to both ω_{eg} and ω_{fe} transitions. Stimulated emission can thus be neglected.
- (3) The spontaneous modes have different frequencies. Modes \mathbf{k}_2 and \mathbf{k}_3 are resonant with ω_{fe} and ω_{eg} respectively.

Diagram (C1) in Fig.4 satisfies the above conditions. The non-resonant diagrams have been omitted. Using this diagram we obtain the optical field and material SNGF's:

$$\mathbb{E}_{LLRR++}^{(5)}(t_6, t_5, \dots, t_1) = \quad (32)$$

$$N\mathcal{E}_1(t_1)\mathcal{E}_1^*(t_2)\frac{2\pi\hbar\omega_3}{\Omega}\frac{2\pi\hbar\omega_2}{\Omega}\exp(i\omega_3(t_6-t_5))\exp(i\omega_3(t_4-t_3))$$

$$\mathbb{V}_{LLRR--}^{(5)}(t_6, t_5, \dots, t_1) = \quad (33)$$

$$\langle \mathcal{T}V_L^3(t_6)V_R^{3,\dagger}(t_5)V_R^{2,\dagger}(t_4)V_L^2(t_3)V_-^1(t_2)V_-^{1,\dagger}(t_1) \rangle$$

Using equations (32), (33) the incoherent part of the signal in the frequency domain is given by:

$$S_{TPEF}(\omega_1) = \frac{N}{\pi\hbar} |\mathcal{E}_1|^2 \frac{2\pi\hbar(\omega_2)}{\Omega} \frac{2\pi\hbar\omega_3}{\Omega} \Im 2\chi_{LRLR--}^{(5)}(-\omega_3; \omega_3, -\omega_2, \omega_2, \omega_1, -\omega_1)$$

The corresponding SNGF can be calculated using the diagram (C1) in Fig.4:

$$-2\chi_{LRLR--}^{(5)}(-\omega_3; \omega_3, -\omega_2, \omega_2, \omega_1, -\omega_1) =$$

$$= \chi_{LRLRLR}^{(5)}(-\omega_3; \omega_3, -\omega_2, \omega_2, \omega_1, -\omega_1) =$$

$$\frac{1}{5!\hbar^5} \langle g|V_1^\dagger G^\dagger(\omega_g + \omega_1)V_2^\dagger G^\dagger(\omega_g + \omega_1 - \omega_2)V_3 G^\dagger(\omega_g + \omega_1 - \omega_2 - \omega_3)V_3 \times$$

$$G(\omega_g + \omega_1 - \omega_2)V_2 G(\omega_g + \omega_1)V_1^\dagger |g\rangle$$

Expansion in the molecular eigenstates gives the frequency-domain response function in the Kramers-Heisenberg form:

$$-2\chi_{LRLR--}^{(5)}(-\omega_3; \omega_3, -\omega_2, \omega_2, \omega_1, -\omega_1) = \quad (34)$$

$$\frac{1}{5!\hbar^5} \sum_{gg'} |\mu_{g'e}^x \mu_{ef}^x \mu_{fg}^y|^2 \frac{1}{(\omega_1 - \omega_{fg})^2 + \gamma_{fg}^2} \left| \frac{1}{\omega_1 - \omega_2 - \omega_{eg} + i\gamma_{eg}} \right|^2 \delta(\omega_1 - \omega_2 - \omega_3)$$

Equation (34) can be recast in the L, R and $+, -$ representations:

$$\begin{aligned} & \chi_{LRLR--}^{(5)}(-\omega_3; \omega_3, -\omega_2, \omega_2, \omega_1, -\omega_1) = \\ & -\frac{1}{4}\chi_{++-----}^{(5)}(-\omega_3; \omega_3, -\omega_2, \omega_2, \omega_1, -\omega_1) - \\ & -\frac{1}{4}\chi_{++++----}^{(5)}(-\omega_3; \omega_3, -\omega_2, \omega_2, \omega_1, -\omega_1) + \\ & +\frac{1}{4}\chi_{+++-+---}^{(5)}(-\omega_3; \omega_3, -\omega_2, \omega_2, \omega_1, -\omega_1) + \\ & +\frac{1}{4}\chi_{+++++---}^{(5)}(-\omega_3; \omega_3, -\omega_2, \omega_2, \omega_1, -\omega_1) \end{aligned}$$

Unlike TPIF, TPEF signal does not depend on the CRF $\chi_{+-----}^{(5)}$. Only other types of the response function contribute. The TPEF is solely determined by the various moments of the molecular fluctuations.

4.1. Type I PDC

We now turn to the coherent response from a collection of identical molecules which interact with one classical pumping mode to spontaneously generate two quantum modes (See Fig.4 (A,B)) with the same polarization. This Type I parametric down conversion (PDC) process is widely used for producing entangled photon pairs. Spontaneously generated modes are emitted into two collinear cones as shown in Fig.4(A). Hereafter we assume perfect phase matching $\Delta\mathbf{k} = \mathbf{k}_1 - \mathbf{k}_2 - \mathbf{k}_3$ which is the case for a sufficiently large sample [1].

The initial conditions for PDC are the same as for TPEF and most PDC experiments are well described by the CRF $\chi_{+--}^{(2)}$. Therefore one would expect a connection between TPEF and PDC, similar to that of TPIF and homodyne-detected SFG. However, as we are about to demonstrate, the causal second order response function does not provide complete description of the PDC process.

To compute corrections to the second order CRF caused by the quantum origin of the spontaneous modes. To do so we again resort to the CTPL diagrams (See Fig.4 (C2)). For the coherent response from the molecular pairs, the optical field SNGF is given by equation (32) with the factor N replaced by $N(N-1)$. The material SNGF (33) can be factorized into the product of conjugate SNGF's for the first and second molecule of the pair as shown in Fig.4 (C2):

$$\begin{aligned} & 2\mathbb{V}_{LRLR--}^{(5)}(t_6, t_5, \dots, t_1) = \tag{35} \\ & \langle \mathcal{T}V_L^3(t_6)V_L^2(t_3)V_L^{1,\dagger}(t_1) \rangle_1 \langle \mathcal{T}V_R^{3,\dagger}(t_5)V_R^{2,\dagger}(t_4)V_R^1(t_2) \rangle_2 \end{aligned}$$

Note that this factorization is unique since $\langle \mathcal{T}V_L^3(t_6)V_R^{2,\dagger}(t_4)V_L^{1,\dagger}(t_1) \rangle = 0$ when the material is initially in its ground state. Using this factorization the coherent PDC signal in the frequency domain can be written as:

$$\begin{aligned} & S_{PDC}(\omega_1, \omega_2) = \tag{36} \\ & \frac{N(N-1)}{4\pi\hbar} |\mathcal{E}_1|^2 \frac{2\pi\hbar\omega_2}{\Omega} \frac{2\pi\hbar(\omega_1 - \omega_2)}{\Omega} |2^{1/2}\chi_{LL-}^{(2)}(-(\omega_1 - \omega_2); -\omega_2, \omega_1)|^2 \end{aligned}$$

Here the generalized response function expanded in the eigenstates has form:

$$2^{1/2} \chi_{LL-}^{(2)}(-(\omega_1 - \omega_2); -\omega_2, \omega_1) = \chi_{LLL}^{(2)}(-(\omega_1 - \omega_2); -\omega_2, \omega_1) = \frac{1}{2! \hbar^2} \frac{\mu_{gf}^y \mu_{fe}^x \mu_{eg}^x}{(\omega_1 - \omega_{gf} + i\hbar\gamma_{gf})(\omega_1 - \omega_2 - \omega_{eg} + i\hbar\gamma_{eg})}$$

This mixed representation can be recast in the +, - representation:

$$\chi_{LL-}^{(2)} = \frac{1}{2} (\chi_{+--}^{(2)} + \chi_{++-}^{(2)}) \quad (37)$$

Comparing the CRF for heterodyne detected DFG (18) and the SNGF's for Type I PDC (37) we see that the latter is described not only by CRF $\chi_{+--}^{(2)}$ but also by the second moment of material fluctuations $\chi_{++-}^{(2)}$. In the L, R representation it selects one Liouville pathway $\chi_{LLL}^{(2)}$, while the classical optical fields drive the material system along all possible pathways.

The SNGF formalism suggests that Type I PDC can be calculated by using the effective interaction Hamiltonian (44) with the material parameter: $\chi^{(2)} = \chi_{LLL}^{(2)}(-(\omega_1 - \omega_2); -\omega_2, \omega_1)$.

Concluding this section we give the signal for the three wave process involving one classical and two quantum fields (CQQ) which contains both an incoherent and a coherent component:

$$S_{CQQ}^{(5)}(\omega_2, \omega_1) = \frac{1}{\pi \hbar} |\mathcal{E}_1|^2 \frac{2\pi \hbar \omega_2}{\Omega} \frac{2\pi \hbar \omega_3}{\Omega} \times \quad (38)$$

$$N \Im 2 \chi_{LRLR--}^{(5)}(-\omega_3; \omega_3, -\omega_2, \omega_2, \omega_1, -\omega_1) +$$

$$+ N(N-1) |2^{1/2} \delta(\omega_3 + \omega_2 - \omega_1) \chi_{LL-}^{(2)}(-\omega_3; -\omega_2, \omega_1)|^2$$

5. Type II PDC; polarization entanglement.

In Type II parametric down-conversion, the two spontaneously-generated photons have orthogonal polarizations. Because of birefringence, the photons are emitted along two non-collinear spatial cones known as ordinary and extraordinary beams (See Fig.5 (A)). Polarization-entangled light [1, 26] is generated at the intersections of the cones. An x polarization filter and a detector are placed at one of the cones intersections. The detector cannot tell from which beam a photon originates. The process involves five optical modes: one classical $|1\rangle|y\rangle$ and four quantum modes $\{|2\rangle|x\rangle, |2\rangle|y\rangle, |3\rangle|x\rangle, |3\rangle|y\rangle\}$.

The polarization-entangled signal is described by CTPL diagrams shown in Fig.5 (C). The Type II PDC signal has two contributions $S_{PDCII}^{(5)} = S_{3x}^{(5)} + S_{2x}^{(5)}$. The signal $S_{3x}^{(5)}$ assumes the form of equation (36), with the material pathway depicted

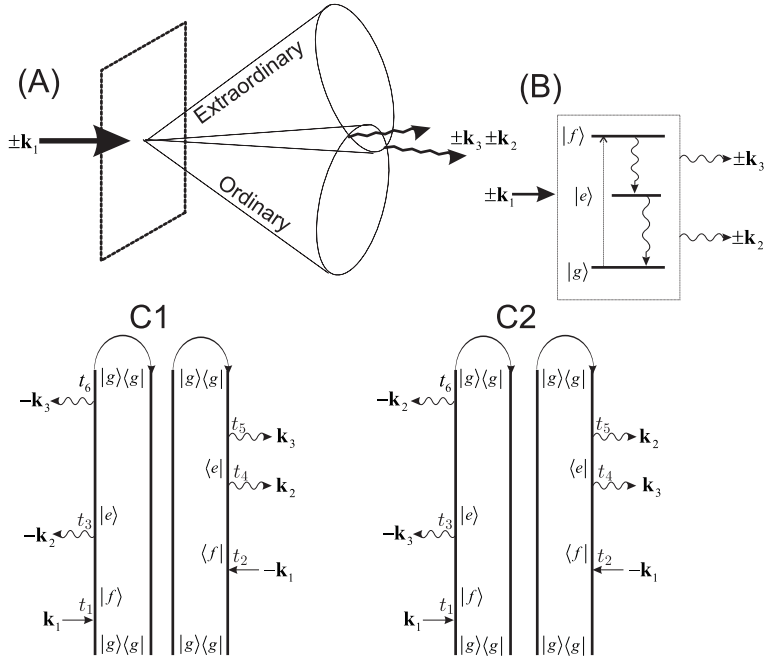


Figure 5. Type II PDC: (A) phase matching, (B) molecular level scheme; (C) CTPL diagrams for the coherent signal from \mathbf{k}_3 (C1) and \mathbf{k}_2 (C2) modes polarized along x direction.

in Fig.5(C1):

$$\begin{aligned}
 & \chi_{LL-}^{(2)}(-(\omega_1 - \omega_2); -\omega_2, \omega_1) = \tag{39} \\
 & = \frac{1}{2} \left[\chi_{+--}^{(2)}(-(\omega_1 - \omega_2); -\omega_2, \omega_1) + \chi_{++-}^{(2)}(-(\omega_1 - \omega_2); \omega_2, -\omega_1) \right] = \\
 & = \frac{1}{2! \hbar^2} \frac{C}{(\omega_1 - \omega_{gf} + i\hbar\gamma_{gf})(\omega_1 - \omega_2 - \omega_{eg} + i\hbar\gamma_{eg})}
 \end{aligned}$$

where the coefficient C is given by:

$$\begin{aligned}
 C^2 = & |\mu_{gf}^y|^2 (|\mu_{fe}^x|^2 |\mu_{eg}^x|^2 + 2\mu_{fe}^x \mu_{eg}^x \mu_{fe}^y \mu_{eg}^y + \tag{40} \\
 & \mu_{fe}^x \mu_{eg}^x \mu_{fe}^y \mu_{eg}^y + \mu_{fe}^y \mu_{eg}^y \mu_{fe}^x \mu_{eg}^x)
 \end{aligned}$$

The signal $S_{3x}^{(5)}$ is described by diagrams (C2) in Fig.5:

$$\begin{aligned}
 & \chi_{LL-}^{(2)}(-\omega_2; -(\omega_1 - \omega_2), \omega_1) = \tag{41} \\
 & = \frac{1}{2} (\chi_{+--}^{(2)}(-\omega_2; -(\omega_1 - \omega_2), \omega_1) + \chi_{++-}^{(2)}(-\omega_2; -(\omega_1 - \omega_2), \omega_1)) = \\
 & = \frac{1}{2! \hbar^2} \frac{C}{(\omega_1 - \omega_{gf} + i\hbar\gamma_{gf})(\omega_2 - \omega_{eg} + i\hbar\gamma_{eg})}
 \end{aligned}$$

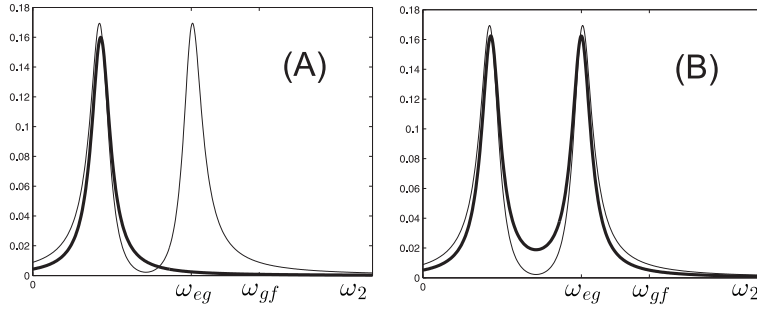


Figure 6. (A) The Type I PDC signal (36) is given by the SNGF (thick solid line) and by the standard causal response function (thin solid curve). (B) Type II PDC signal (42) given by the SNGF's (thick solid line) is compared with the signal given by the causal response function (thin solid curve). The perfect matching conditions are assumed and the classical beam frequency is set into resonance with ω_{gf} (for parameters see the text). The signal dependence on ω_2 is presented.

The total Type II PDC signal is:

$$S_{PDCII}(\omega_1) = \tag{42}$$

$$\frac{N(N-1)}{4\pi\hbar} |\mathcal{E}_1|^2 \frac{2\pi\hbar\omega_2}{\Omega} \frac{2\pi\hbar(\omega_1 - \omega_2)}{\Omega} \times$$

$$\left[|2^{1/2} \chi_{LL-}^{(2)}(-(\omega_1 - \omega_2); -\omega_2, \omega_1)|^2 + |2^{1/2} \chi_{LL-}^{(2)}(-\omega_2; -(\omega_1 - \omega_2), \omega_1)|^2 \right]$$

We shall compare the generalized response given by the SNGF's ($\chi_{+--}^{(2)} + \chi_{++-}^{(2)}/2$) in equation (41) with the CRF $\chi_{+--}^{(2)}$ (see equation (18)) commonly used to describe both types of PDC. We assume a model material system with the following parameters. The transition dipole moments are $\mu_{gf}^y = \mu_{fe}^x = \mu_{eg}^x = 0.1$ and $\mu_{eg}^y = \mu_{fe}^y = 0$ (arbitrary units). For all transitions the dephasing rates are the same $\hbar\gamma_{gf} = \hbar\gamma_{eg} = 0.05\omega_{gf}$. The classical mode \mathbf{k}_1 provides a common factor for causal and generalized response function:

$$\frac{|\mu_{gf}|^2}{\omega_1 - \omega_{gf} + i\hbar\gamma_{fg}}$$

Hence, without we can assume it to be in resonance with the $\omega_1 \approx \omega_{gf}$ transition.

In Type II PDC the SNGF's approach and conventional CRF description give quantitatively similar results as both resonances ($\omega_2 \approx \omega_{eg}$ and $\omega_1 - \omega_2 \approx \omega_{eg}$) participate (See Fig.6 (A)). On the other hand, Type I PDC has only one resonance in the SNGF $\omega_1 - \omega_2 \approx \omega_{eg}$, and therefore it is qualitatively different from the CRF near the resonance (See Fig.6(B)). The off-resonant regime is well described by the CRF.

6. Conclusions

In quantum optics, a three wave mixing process is commonly described by an effective interaction Hamiltonian for the radiation modes[12]. For SFG this reads:

$$H_{eff} = - \int d\mathbf{r} \chi^{(2)} E_3^\dagger(\omega_1 - \omega_2) E_2^\dagger(\omega_2) E_1(\omega_1) \tag{43}$$

and for DFG and PDC:

$$H_{eff} = - \int d\mathbf{r} \chi^{(2)} E_3^\dagger(\omega_1 + \omega_2) E_2(\omega_2) E_1(\omega_1) \quad (44)$$

The second order nonlinearity tensor $\chi^{(2)}$ is responsible for the coupling between the modes in both cases. Various techniques differ by the initial state of the fields. The nonlinearity tensor contains various second order susceptibilities $\chi_{+--}^{(2)}$. Latter is based on assumption that the molecular response is classical. That is it is described by causal response function (CRF) and optical fields are not affected by material fluctuations. However, this assumption justified only when *all* optical modes are in coherent classical states; adding (subtracting) a single photon to such modes makes no noticeable effect.

Here we considered techniques which involve optical modes initially in the vacuum state. The changes in their state due to material fluctuations must be taken into account. These processes can not be described by the conventional causal response function. The parametric model (equations (43) and (44)) must be adjusted to incorporate non-causality by treating both light and matter quantum mechanically.

A unified framework for calculating non-linear optical signals generated in a material system by interactions with any combination of quantum and classical radiation fields is provided by The SNGF formalism developed in this article. SNGF formalism incorporates CRF and reduces to the latter in case when the coherent optical fields as shown here for heterodyne-detected SFG and DFG techniques. CRF contains all possible molecular Liouville pathways. In SNGF formalism this statement is proved by switching from $+$, $-$ to L , R representations of the SNGF's. When quantum optical fields are involved the number of available pathways may be reduced. This, in turn, makes various moments of molecular fluctuations to play essential role in the non-linear signal. Here we prove this statement by switching from L , R to $+$, $-$ representation. Various spectroscopic techniques which involve both quantum and classical optical fields were considered.

We have examined the applicability of the conventional second order parametric model for the description of the PDC and homodyne-detected SFG, since the processes involve highly non-classical spontaneously generated modes. We compared the incoherent TPEF and the coherent PDC signals. The incoherent TPIF was compared with the coherent homodyne-detected SFG. The second order parametric model does not apply to a single molecule incoherent response and has to be extended to the fifth order generalized response function description. Two photon fluorescence with one quantum and two classical modes (TPIF) is described not only by the causal response function $\chi_{+-----}^{(5)}$ but also by the second moment of molecular fluctuation $\chi_{++-----}^{(5)}$. The two photon fluorescence signal with two quantum and one classical modes (TPEF) does not contain the causal response function but involves higher moments in material fluctuations $\chi_{++++---}^{(5)}$, $\chi_{+++++-}^{(5)}$.

For ensembles of identical molecules, such as crystals with no inversion symmetry, the SNGF corresponding to TPIF can be reduced to the homodyne-detected SFG given by ordinary second order response function $\chi_{+--}^{(2)}$. PDC is the coherent analogue of TPEF. In addition to the CRF $\chi_{+--}^{(2)}$, PDC contains contributions from the second moment of molecular fluctuations $\chi_{+++-}^{(2)}$.

Equations (31) and (38) represent closed compact expressions for both coherent and incoherent signals with one and two quantum modes respectively. In the off-resonant regime, both types of PDC are well described by conventional second

order CRF. Quantum corrections quantitatively affect the Type II PDC but bring qualitative changes into Type I PDC in the vicinity of molecular resonances.

In this paper we considered only one type of nonclassical optical fields - spontaneously emitted photons. Future applications to other types of non-classical fields such as, for instance, entangled photons, are of great interest [29]. The SNGF formalism show that non-causal contributions to the non-linear signals are signatures of various moments of molecular fluctuations. For clarity of the presentation

Finally we summarize the advantages of the SNGF's formalism:

- Processes involving an arbitrary number of classical and quantum modes of the radiation field may be treated within the same framework by simply varying the number of + and - superoperators.
- Intuitive loop diagrams can be used to describe all processes in the L, R representation.
- Incoherent and coherent (cooperative) signals may be derived from the same expressions.
- A unified approach is provided for resonant and off-resonant measurements. Only the latter may be described by an effective Hamiltonian for the field which depends parametrically on the matter.
- Nonlinear spectroscopy conducted with resonant classical fields only accesses the CRF. Quantum fields reveal the broader family of SNGF's which carry additional information about fluctuations as shown in Table C1.
- Spectroscopy with quantum entangled fields [27, 28] may be naturally described by the SNGF formalism.

Acknowledgments

This work was supported by the National Science Foundation Grant CHE-0745892 and National Institutes of Health Grant GM59230.

References

- [1] C. Gerry and P. Knight, *Introductory Quantum Optics* (Cambridge University Press, 2005).
- [2] M. Scully and M. Zubairy, *Quantum Optics* (Cambridge University Press, 1997).
- [3] R. Glauber, *Quantum Theory of Optical Coherence: Selected Papers and Lectures* (Wiley-VCH, 2007).
- [4] S. Mukamel, *Principles of nonlinear optical spectroscopy* (Oxford University Press New York, 1995).
- [5] N. Bloembergen, *Nonlinear Optics* (World Scientific, 1996).
- [6] A.E. Cohen and S. Mukamel, Resonant Enhancement and Dissipation in Nonequilibrium van der Waals Forces, *Phys. Rev. Lett.* **91** (23), 233202 (2003).
- [7] U. Harbola, J. Maddox and S. Mukamel, Nonequilibrium superoperator Greens function approach to inelastic resonances in STM currents, *Physical Review B* **73** (20), 205404 (2006).
- [8] C.A. Marx, U. Harbola and S. Mukamel, Nonlinear optical spectroscopy of single, few, and many molecules: Nonequilibrium Green's function QED approach, *Physical Review A* **77** (2), 022110 (2008).
- [9] U. Harbola and S. Mukamel, Superoperator nonequilibrium Green's function theory of many-body systems. Applications to charge transfer and transport in open junctions, *Physics Reports* **465** (5), 191, (2008).
- [10] Y. Shen, Surface properties probed by second-harmonic and sum-frequency generation, *Nature* **337** (6207), 519-525 (1989).
- [11] B. Dick and R. Hochstrasser, Spectroscopic and line-narrowing properties of resonant sum and difference frequency generation, *The Journal of Chemical Physics* **78**, 3398 (1983).
- [12] L. Mandel and E. Wolf, *Optical Coherence and Quantum Optics* (Cambridge University Press, 1995).
- [13] C.K. Hong and L. Mandel, Theory of parametric frequency down conversion of light, *Phys. Rev. A* **31** (4), 2409-2418 (1985).
- [14] D. Klyshko, *Photons and Nonlinear Optics* (Gordon and Breach New York, 1988).
- [15] W.H. Louisell, A. Yariv and A.E. Siegman, Quantum Fluctuations and Noise in Parametric Processes, *Phys. Rev.* **124** (6), 1646-1654 (1961).
- [16] K. Edamatsu, Entangled Photons: Generation, Observation, and Characterization, *Japanese Journal of Applied Physics* **46** (11), 7175 (2007).
- [17] A. URen, R. Erdmann, M. de la Cruz-Gutierrez and I. Walmsley, Generation of Two-Photon States with

- an Arbitrary Degree of Entanglement Via Nonlinear Crystal Superlattices, *Physical Review Letters* **97** (22), 223602 (2006).
- [18] W. Denk, J. Strickler and W. Webb, Two-photon laser scanning fluorescence microscopy, *Science* **248** (4951), 73–76 (1990).
- [19] C. Xu and W. Webb, Measurement of two-photon excitation cross sections of molecular fluorophores with data from 690 to 1050 nm, *J. Opt. Soc. Am. B* **13** (3), 481–491 (1996).
- [20] P.R. Callis, On the theory of two-photon induced fluorescence anisotropy with application to indoles *The Journal of Chemical Physics* **99**, 27–37 (1993).
- [21] A. Rehms and P. Callis, Two-photon fluorescence excitation spectra of aromatic amino acids, *Chemical physics letters* **208** (3-4), 276–282 (1993).
- [22] U. Harbola, J. Maddox and S. Mukamel, Many-body theory of current-induced fluorescence in molecular junctions, *Physical Review B* **73** (7), 75211 (2006).
- [23] D. Andrews and P. Allcock, *Optical harmonics in molecular systems* (Wiley-VCH Weinheim, 2002).
- [24] T. Chui and K. Wong, Study of hyper-Rayleigh scattering and two-photon absorption induced fluorescence from crystal violet, *The Journal of Chemical Physics* **109**, 1391 (1998).
- [25] C. Xu, J. Shear and W. Webb, Hyper Rayleigh and hyper Raman scattering background of liquid water in two photon excited fluorescence detection, *Anal. Chem* **69**, 1285–1287 (1997).
- [26] M.H. Rubin, D.N. Klyshko, Y.H. Shih and A.V. Sergienko, Theory of two-photon entanglement in type-II optical parametric down-conversion, *Phys. Rev. A* **50** (6), 5122–5133 (1994).
- [27] D. Lee and T. Goodson, Entangled Photon Absorption in an Organic Porphyrin Dendrimer, *Journal of physical chemistry. B, Condensed matter, materials, surfaces, interfaces, & biophysical chemistry* **110** (51), 25582–25585 (2006).
- [28] A. Pe'er, B. Dayan, A.A. Friesem and Y. Silberberg, Temporal Shaping of Entangled Photons, *Physical Review Letters* **94**, 073601 (2005).
- [29] O. Roslyak, S. Mukamel, Photon Entanglement Signatures in Homodyne-Detected Difference-Frequency-Generation, *Optics express*, (2009).

Appendix A. Superoperator algebra

Below we briefly summarize superoperators and their algebraic properties [8].

The superoperators are defined by their action on an ordinary operator X :

$$A_- X = \frac{1}{\sqrt{2}} [A, X] \quad (\text{A1})$$

$$A_+ X = \frac{1}{\sqrt{2}} (AX + XA) \quad (\text{A2})$$

The following properties can be verified directly from the definition:

$$\langle AX \rangle = \langle A_+ X \rangle; \quad \langle A_- X \rangle = 0 \quad (\text{A3})$$

$$(AB)_- = A_- B_+ + A_+ B_-; \quad (AB)_+ = A_+ B_+ + A_- B_- \quad (\text{A4})$$

The L(left),R(right) superoperators are given by their action in the Hilbert space:

$$A_L X = AX \quad A_R X = XA$$

The L, R and $+, -$ superoperators are related by the unitary transformation:

$$A_- = \frac{1}{\sqrt{2}} (A_L - A_R) \quad A_+ = \frac{1}{\sqrt{2}} (A_L + A_R)$$

$$A_L = \frac{1}{\sqrt{2}} (A_+ - A_-) \quad A_R = \frac{1}{\sqrt{2}} (A_+ + A_-)$$

Appendix B. Rules for the CTPL diagrams

The following rules are used to construct the loop diagrams [8]:

- (1) Time runs along the loop clockwise from bottom left to bottom right.
- (2) The left branch of the loop represents the ket, the right represents the bra.
- (3) Each interaction with a field mode is represented by a line acting on either the right (R-operators) or the left (L-operators) branch.
- (4) The field is marked by dressing the lines with arrows, where an arrow pointing to the right (left) represents the field annihilation (creation) operator $E_\alpha(t)$ ($E_\alpha^\dagger(t)$).
- (5) Within the RWA, each interaction which annihilates a photon $E_\alpha(t)$ is accompanied by the operator V_α^\dagger , which leads to molecular excitation. Similarly $E_\alpha^\dagger(t)$ de-excites the molecule by applying operator V .
- (6) Arrows pointing "inwards" (i.e. pointing to the right on the ket and to the left on the bra) consequently cause absorption of a photon by exciting the system, whereas arrows pointing "outwards" (i.e. pointing to the left on the bra and to the right on the ket) represent deexciting the system by photon emission.
- (7) The observation time t_{m+1} , is fixed and is always chronologically the last. As a convention, it is chosen to occur from the left. This can always be achieved by a reflection of all interactions through the center line between the ket and the bra, which corresponds to taking the complex conjugate of the original correlation function.
- (8) The loop translates into an alternating product of interactions (arrows) and free evolutions periods (vertical solid lines) along the loop.
- (9) Since the loop time goes clockwise along the loop, periods of free evolution on the left branch amount to propagating forward in real time with the propagator give by the retarded Green's function G . Evolution on the right branch corresponds to backward propagation (advanced Green's function G^\dagger).
- (10) The frequency arguments of the various propagators are cumulative, i.e. they are given by the sum of all "earlier" interactions along the loop. Additionally, the ground state frequency is added to all arguments of the propagators.
- (11) The Fourier transform of the time-domain propagators adds an additional factor of $i(-i)$ for each retarded (advanced) propagator.
- (12) The overall sign of the SNGF is given by $(-1)^{N_R}$, where N_R is the number of R superoperators.

Appendix C. Table I

Three wave processes						
Heterodyne			Homodyne			
Technique	SFG	DFG	TPIF	TPEF	SFG	Coherent
Modes	$c/c/c$	$c/c/c$	$c/c/q$	$c/q/q$	$c/c/q$	PDC
ω_3	$\omega_1 + \omega_2$	$\omega_1 - \omega_2$	-	-	$\approx \omega_1 + \omega_2$	$\approx \omega_1 - \omega_2$
Argument	$(-\omega_3; \omega_2, \omega_1)$	$(-\omega_3; -\omega_2, \omega_1)$	$(-\omega_3; \omega_3, \omega_2, -\omega_2, \omega_1, -\omega_1)$	$(-\omega_3; \omega_3, -\omega_2, \omega_2, \omega_1, -\omega_1)$	$(-\omega_3; \omega_2, \omega_1)$	$(-\omega_3; -\omega_2, \omega_1)$
SNGF's +, -	$\chi_{+---}^{(2)}$	$\chi_{+---}^{(2)}$	$\chi_{++++}^{(5)}$ $-\chi_{+---}^{(5)}$	$-\chi_{++++}^{(5)}$ $+\chi_{+---}^{(5)}$	$ \chi_{+---}^{(2)} ^2$	$ \chi_{+---}^{(2)} + \chi_{+++}^{(2)} ^2$
SNGF's mixed	-	-	$\chi_{LR}^{(5)}$ $\chi_{LRL}^{(5)}$	$\chi_{LRLR}^{(5)}$	-	-
SNGF's L, R	$\chi_{LLL}^{(2)}$	$\chi_{LLL}^{(2)}$ $-\chi_{LRL}^{(2)}$	$\chi_{LRLRLR}^{(5)}$	$-\chi_{LRLRLR}^{(5)}$	$ \chi_{LLL}^{(2)} ^2$	$ \chi_{LLL}^{(2)} ^2$
Expression	eq.(20)	eq.(18)	eq.(26)	eq.(34)	eq.(20)	eq.(36); eq.(39), (41)

Table C1. SNGF's for three wave mixing techniques: heterodyne-detected SFG and DFG with all classical modes (c); incoherent TPIF with two classical and one quantum (q) mode and corresponding coherent homodyne-detected SFG; incoherent TPEF with one classical and two quantum modes and Type I PDC; Type II PDC SNGF with one classical and four quantum modes.